Research Article

Weihong Guo, Shucai Liu*, Yaoning Liu, and Shuangshuang Chen

Application of electrical resistivity imaging to detection of hidden geological structures in a single roadway

https://doi.org/10.1515/geo-2020-0175
received September 23, 2019; accepted June 17, 2020

Abstract: Locating concealed geological structures in coal seams on both sides of a coal mine excavation roadway is of vital importance for safe production. Conventional electrical resistivity imaging methods mostly arrange observation systems on the roadway roof and floor, so they are inevitably deficient when it comes to detecting concealed geological structures in coal seams. According to the electric field distribution characteristics of artificial field sources for electrical resistivity imaging methods and utilizing the shielding of current by roadway cavities, this paper proposes the parallel coal seam detection method that arranges observation systems in coal seams on the roadway side to detect concealed geological structures in coal seams. On the basis of introducing the principles of consequent detection methods, this paper investigates the influence of roadway cavities on observation results and offers a method of correcting the influence of roadway cavities. In view of the geoelectric characteristics of typical concealed geological structures in working faces, this paper establishes numerical models to verify the feasibility of the parallel coal seam detection method. As indicated by the calculation results, the consequent pole–dipole (A-MN) observation system is the most ideal in terms of dividing the geoelectric interfaces of concealed geological structures in working faces, and its detection effect is influenced significantly by the coal seam thickness and the electric differences between surrounding rock and anomalous bodies. Coal seam resistivity slightly influences detection of the consequent pole–dipole system. According to practical application effects, the parallel coal seam detection method can solve the problem of detecting concealed geological structures in "single-roadway" working faces.

Keywords: electrical resistivity imaging method, parallel coal seam detection method, roadway cavity affect, forward calculation

1 Introduction

Faults, collapse columns, and other concealed geological structures existing in coal seams not only jeopardize coal seam continuity and affect roadway and working face layout but are also extremely apt to cause water inrush or coal and gas outburst accidents when connected with an aquifer or a gas enrichment area. Thus, conducting a thorough investigation into concealed geological structures in coal seams is crucial for guiding working face layout and water control in coal mines.

In recent years, focusing on the differences between surrounding rock and concealed geological structures in coal strata in terms of electric properties, magnetic property, wave impedance, and other physical properties, a series of geophysical prospecting techniques have developed rapidly [1], primarily including: (1) ground electromagnetic methods that include: the DC electrical sounding method [2–5], high-density resistivity method [6], and ground transient electromagnetic method [7]. Methods of these types uniformly arrange field sources and receivers on the ground surface, have poor coupling with targets, and can satisfactorily resolve power shallow anomalous bodies; however, with increasing depth, the resolution drops rapidly [8]. (2) Mine perspective methods that include: the radio wave penetration method [9], the channel wave perspective method [10,11], and the DC penetration method [12]. Methods of

* **Corresponding author: Shucai Liu,** Institute of Mine Water Hazards Prevention and Controlling Technology, School of Resources and Geosciences, China University of Mining and Technology, Xuzhou, Jiangsu Province, 221116, China, e-mail: cumtlsc@126.com
Weihong Guo, Yaoning Liu: Institute of Mine Water Hazards Prevention and Controlling Technology, School of Resources and Geosciences, China University of Mining and Technology, Xuzhou, Jiangsu Province, 221116, China
Shuangshuang Chen: ChangJiang Geophysical Exploration & Testing Co., Ltd (Wuhan), Wuhan, Hubei Province, 430010, China

these types generally carry out construction between two adjacent roadways of a working face and are characterized by close targets, sound coupling performance, and a high resolution [13]; however, mine perspective methods are susceptible to restriction by roadway conditions and do not apply to "single-roadway" working faces with only one available roadway. (3) In-seam seismic survey includes transmission and reflection. Transmission, the source, and detector are arranged in different roadways, respectively. The source is excited in one roadway and the detector receives in-seam waves in the other roadway. Reflection, the source, and the detector are arranged in a tunnel or on the working surface [14–16]. Its construction efficiency is low, the cost is high, and as the source, the use of explosives is strictly controlled. The mine transient electromagnetic method is introduced to mine applications via the ground transient electromagnetic method and has the advantages of convenient construction and high sensitivity to low-resistivity bodies. The mine transient electromagnetic method is affected by the volume effect, has a low resolution, has difficulties in accurately identifying practical geoelectric interfaces, and is generally used to detect the stratum water abundance [17,18]. (4) In-seam electrical resistivity imaging methods: Given that detection results in different directions are closely related to the electric characteristics of mediums adjacent to the electrodes, an all-round prospecting can be conducted on concealed geological structures in coal measure strata [19–21].

Since the in-seam resistivity experiment carried out in 1958 by the Department of Geological Prospecting under the Ministry of Coal Industry, many scholars have examined electrical resistivity imaging methods by means of theoretical analysis, numerical simulation, physical simulation, and engineering practice. Li focused on the DC layer sounding method and used it to trace the extension of geological structures with exposed roadways in coal seams. Yue used in-seam electrical resistivity imaging to detect seam floor water-flow and water-bearing structures and analyzed the influence of roadway cavities on detection results, achieving satisfactory application effects [22]. Liu put forward a 3D parallel electrical survey-based prospecting technique and used the spatial layout observation system of roadways in the vicinity of working faces to detect seam roof and floor concealed structures. Liu examined the evolution of seam floor water-flow fissures using electrical resistivity imaging methods and designed a dynamic monitoring system for monitoring seam floor water-flow fissure zones [23]. On the basis of the finite element numerical simulation, Zhang concentrated on the technique of full-space advanced focus detection with DC resistivity in tunnels and used it to detect head-on unfavorable geological bodies [24].

To sum up, existing in-seam electrical resistivity imaging methods mostly arrange observation systems on single or adjacent roadway roof and floor to detect concealed structures, so they are inevitably deficient when it comes to detecting concealed geological structures in coal seams [25]. According to electric field distribution characteristics of artificial field sources in electrical resistivity imaging methods and utilizing the current shielding of the roadway cavity, this paper proposes a detection method that arranges observation systems in coal seams on the roadway side to detect concealed geological structures in "single-roadway" working faces. On the basis of introducing the principles of consequent detection methods, this paper analyzes the correlation between the roadway cavity, coal seam thickness, coal seam resistivity, and surrounding rock resistivity with observation results. Finally, this paper applies the consequent detection method to practical engineering detection.

2 Method

2.1 Basic principles

The parallel coal seam detection method arranges observation systems in coal seams to collect data, Figure 1(a). Because of the shielding of current by the roadway cavity, the majority of supply current flows into the working face, and the potential difference measured primarily contains information on geoelectric anomalies in the working face. In practice, two electric parameters from electrical resistivity imaging methods are generally calculated using equation (1) according to the potential difference ΔU_{MN} between the electrodes and the relative positions of the electrodes [26–28].

$$\begin{cases} \rho = \dfrac{\Delta U_{MN}}{I} \\ \rho_s = K\dfrac{\Delta U_{MN}}{I} \end{cases} \tag{1}$$

where ΔU_{MN} denotes the potential difference between the electrodes, mV; I denotes the supply current intensity, mA; K denotes the array coefficient.

In coal measures, coal seams and their roof and floor strata are composed of layered mediums with different electric properties. For the simple three-layer geoelectric model shown in Figure 1(b), the potential expression of a point source in full space can be solved using the image method:

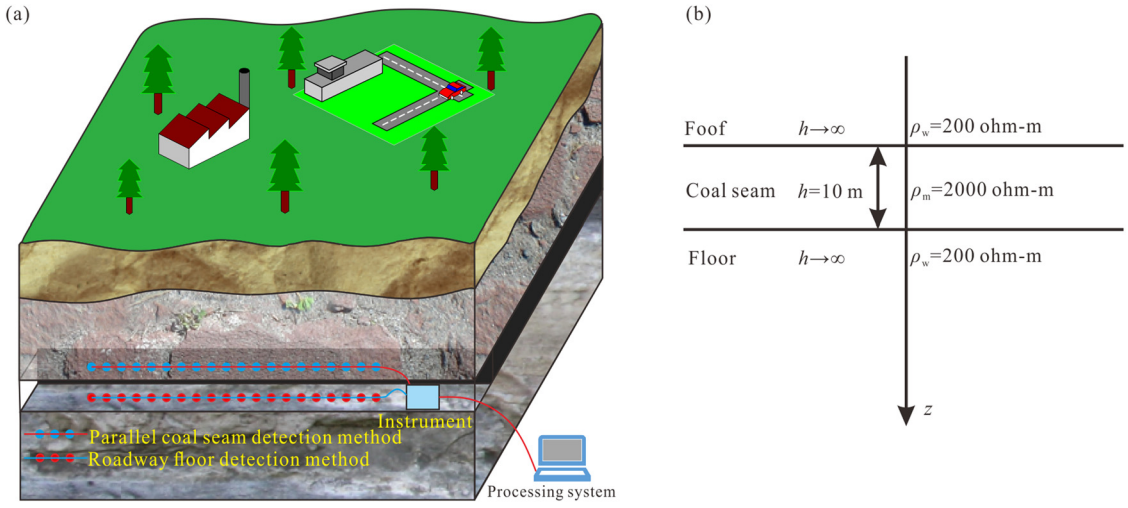

Figure 1: (a) Schematic diagram of the observation system layout and (b) a three-layer geoelectric model.

$$U_{ij}(r,z) = \frac{I\rho_j}{4\pi}\int_0^{\infty}[a_{ij}e^{-\lambda|z|} + b_{ij}e^{-\lambda z} + c_{ij}e^{\lambda z}]J_0(\lambda r)\mathrm{d}\lambda \quad (2)$$

where (r,z) denotes the coordinates of the measuring point in cylindrical coordinates; i denotes the number of medium in which a point source is located; j denotes the number of medium in which an observation point is located; a_{ij}, b_{ij}, c_{ij} denote undetermined coefficients, which can be solved using boundary conditions; λ is an integral variable; $J_0(\lambda r)$ is a zero-order Bessel function of the first kind.

Point sources are located in the middle of seam floor and coal seam, respectively, and equation (2) is used to calculate the potential, as shown in Figure 2. It can be known that: (1) the potential isoline distorts the interface of coal strata, but still maintains its continuity. (2) When a field source is located on the seam floor, electric field energy is primarily concentrated in the floor surrounding rock; when a field source is located in the middle of coal seams, the potential isoline presents an approximately elliptical distribution, and more current flows to coal seams. Adopting consequent detection methods obtains more information on geoelectric anomalies in coal seams.

2.2 Observation system design

General working faces are less than 200 m in width ($L <$ 200 m), and, within this prospecting scope, electrical resistivity imaging methods have a high resolution; hence, consequent detection methods can be used to realize the detailed detection of concealed geological structures in "single-roadway" working faces. In the observation system design for the consequent detection method, a close attention should be paid to the following aspects:

(1) Array mode: it is required to guarantee sufficient sensitivity and minimize the "blind area" in prospecting.
(2) Measuring line layout: measuring lines should be arranged with reference to exposed geological structures, and measuring line length should be greater than the length of the target prospecting section.
(3) Parameter selection: polar distance sequence should be determined according to prospecting depth and roadway supporting conditions, guaranteeing both the precision of shallow detection and the accuracy of deep measurement.
(4) Interference suppression: in practical construction, it is necessary to suppress the interference caused by bodies with heterogeneous electric properties (such as the anchor net and anchor rod) and electrode earthing resistance, ensuring signal quality.

3 Numerical simulation

3.1 Geoelectric model establishment

In the primary state, the sedimentary sequence of coal strata is clear, and geoelectric characteristics follow regular variation laws in the longitudinal direction

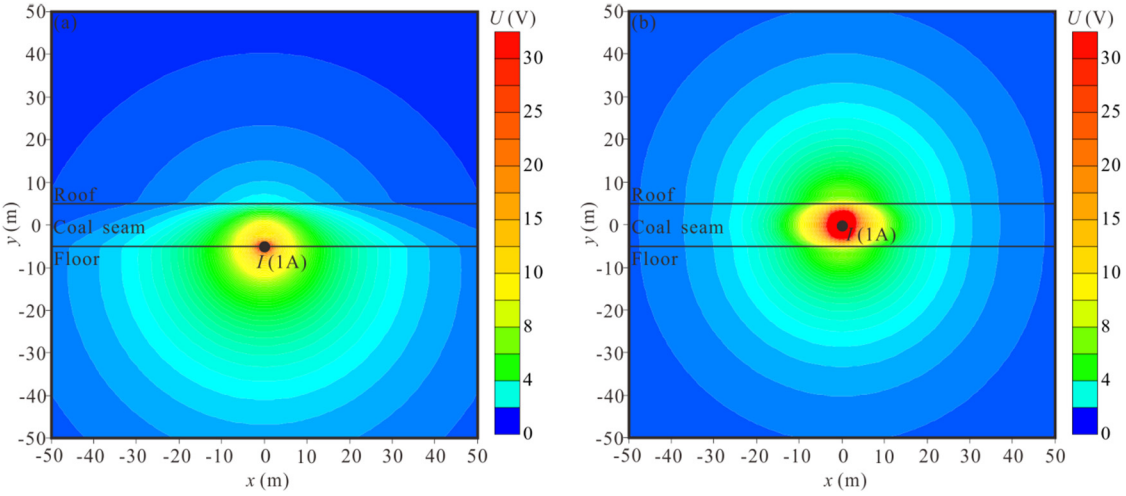

Figure 2: Distribution of the point electric field. (a) Source located in the coal seam floor and (b) source located in the middle of the coal seam.

(generally manifested as a resistivity ranking of mudstone < sandstone < coal seam). In the transverse direction, resistivity distribution is relatively homogeneous. In cases where the geological or groundwater movement causes stratigraphic dislocation, erosion, or caving and forms fault fissure zones, karst caves, collapse columns, or other concealed geological structures, the intrinsic electric variation laws of primary coal measure strata are altered, whether water still present or not. Considering that concealed geological structures commonly found in coal seams are typically collapse columns, they can be abstracted as cuboids in full-space infinitely large mediums, as shown in Figure 3.

Geoelectric models are 600 m (length) × 200 m (width) × 200 m (height) in size. Collapse columns penetrate coal seams, and are developed in both the roof and floor and are 40 m × 40 m × 100 m in size. Measuring lines are arranged in the middle of coal seams. In addition, this paper sets coal seam thickness (roadway height) as h, surrounding rock resistivity as ρ_w, coal seam resistivity as ρ_m, and roadway resistivity as ρ_h.

3.2 Influence correction of the roadway cavity

Given that the parallel coal seam detection method is used in the mine roadway construction, the presence of roadway cavities is bound to cause distortion in full-space steady current fields. In this sense, studying methods for correcting the influence of roadway cavities is vital for data processing and interpretation using consequent detection methods.

For the sake of generality, this paper makes the following assumptions: roof and floor surrounding rock resistivity $\rho_w = 200\ \Omega$ m, coal seam resistivity $\rho_m = 500\ \Omega$ m, roadway cavity resistivity $\rho_h = 1.0 \times 10^{11}\ \Omega$ m, roadway height $h = 5$ m, and roadway width $a = 1, 2, \ldots, 9, 10$ m. A 3D finite element method is used for the forward calculation of geoelectric models of different roadway widths, as shown in Figure 4(a). It can be known that: the roadway cavities have a significant influence on the small polar distance; with increasing polar distance, the influence of roadway cavities on measurement results presents an exponential decay, and apparent resistivity gradually approaches surrounding rock resistivity; with increasing roadway width (section),

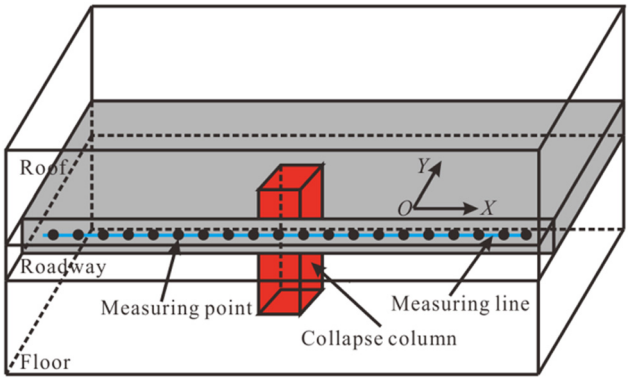

Figure 3: Schematic diagram of the collapse column geoelectric model and line layout.

the influence scope of roadway cavities gradually expands.

To further study methods of correcting the influence of roadway cavities, this paper assumes the relationship between apparent resistivity and full-space apparent resistivity under the influence of roadway cavity as:

$$\begin{cases} \rho_s^a = K_D \rho_s^m \\ K_D = f(S, L) \end{cases} \tag{3}$$

where ρ_s^a denotes the full-space apparent resistivity; ρ_s^m denotes the apparent resistivity under the influence of roadway cavities; K_D denotes the correction coefficient, which is a function of the roadway cross-section area and electrode spacing; S denotes the roadway cross-section area; L denotes the electrode spacing.

In practical applications, electric parameters of surrounding rock and coal seams can be measured in the field and used to establish geoelectric models with/without roadways for the forward calculation of background fields. Next, a ratio operation is performed to obtain the correction coefficient. Finally, full-space apparent resistivity is acquired from the measured apparent resistivity data. Figure 4(b) shows the apparent resistivity curve of the geoelectric model for low-resistivity collapse columns when the roadway width is $a = 5$ m. Clearly, adopting the correction method from equation (3) can effectively suppress the influence of roadway cavities on the small polar distance, and the curve after the roadway cavity correction basically overlaps with the curve without roadway cavities; however, with increasing polar distance, the curve after correction gradually overlaps with the curve with roadway cavities, meaning that the correction method cannot eliminate the influence of roadway cavities on the anomaly response amplitude.

Parallel coal seam detection method arrange observation systems in the middle of coal seams on the roadway side, and roadway cavities (high-resistivity layer) can be seen as a current shielding layer, causing more current to flow into coal seams. Thus, roadway cavities may influence the anomaly response amplitude. Figure 5 shows the apparent resistivity variation rates for a Schlumberger array when collapse columns are located in coal seams and on the outside of the roadway (calculated from equation (4)), respectively. By comparing Figure 5(a) and (b), the shielding of current by roadway cavities increases the anomaly response amplitude in coal seams and weakens the influence of anomalous bodies on the outside of roadway on observation results. That is, roadway cavities enhance the ability of the parallel coal seam detection method to detect concealed geological structures in working faces.

$$\eta(x) = \frac{\rho_s^{abnorm}(x) - \rho_s^{norm}(x)}{\rho_s^{norm}(x)} \tag{4}$$

where η denotes the apparent resistivity variation rate; ρ_s^{abnorm} denotes the apparent resistivity with anomalous bodies; ρ_s^{norm} denotes the apparent resistivity of background field; x denotes the observation point position.

4 Results and discussion

Considering that different array modes have different sensitivities when it comes to the reflection of the same geoelectric conditions, the commonly used DC electrical sounding observation system is adopted to perform the forward calculation of the geoelectric model for the same collapse column using four array modes, i.e.,

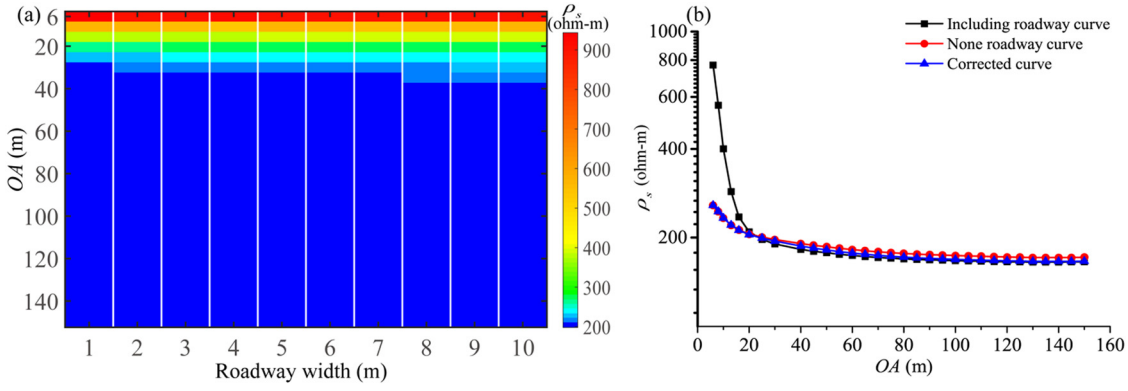

Figure 4: Influence correction of the roadway cavity. (a) Gray-scale map of apparent resistivity for different roadway widths and (b) apparent resistivity curves.

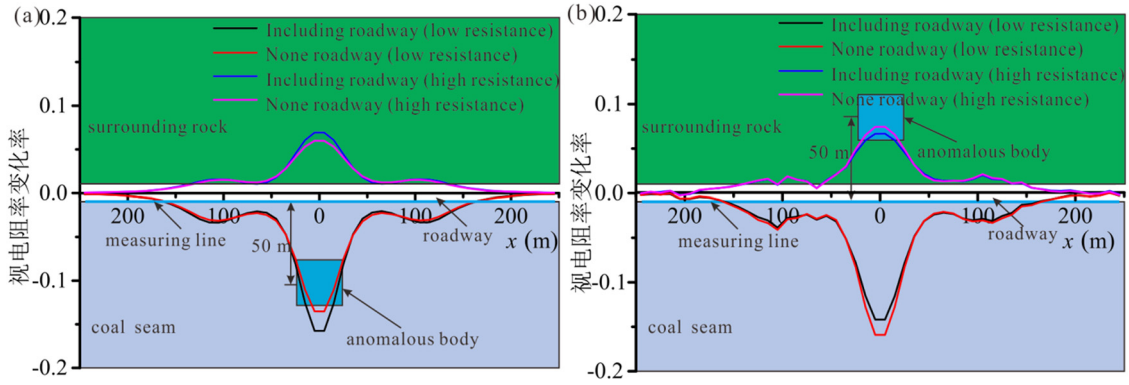

Figure 5: Apparent resistivity section curves of the Schlumberger array (OA = 100 m). (a) Abnormal body located in the coal seam and (b) abnormal body located outside the roadway.

pole–dipole array, Schlumberger array, dipole–dipole array, and differential array. Next, on the basis of the "pseudo-depth" calculation formula given by Edwards (1977) and our working experience, this paper sets $y = 0.6 \times \mathrm{OA}$ to draw apparent resistivity isolines, as shown in Figure 6 (all apparent resistivity isolines represent results obtained after correcting for the influence of roadway cavities according to equation (3)).

Figure 6 shows the apparent resistivity isolines for different array modes, in which the blue box represents the actual plane position of the collapse column. The four array modes are all in a thin-layered high-resistivity state in shallow areas, corresponding to the coal seam resistivity; apparent resistivity isolines show a distortion around anomalous bodies. Comparing Figure 6(a)–(d), the Schlumberger array has a strong volume effect, and the scope of the high-resistivity anomaly area deviates significantly from the actual position of the anomalous body; the differential array is greatly influenced by the coal seam resistivity, and the layered high resistivity in shallow areas shields the anomaly response of the collapse column; the high-resistivity anomaly area in the dipole–dipole array is centered around the collapse column and presents a "parabolic" zonal distribution, making it difficult to separate geoelectric interfaces; affected by"infinite" electrodes, the pole–dipole array is slightly anomalous beside measuring lines and shows an obvious high-resistivity closure area at the actual plane position of the collapse column and, influenced by the development of collapse columns in roof and floor surrounding rock, the high-resistivity anomaly area tends to extend downwards. In addition, practical construction areas are mostly located on the two roadway sides, so the parallel coal seam detection method of electrical resistivity imaging generally uses a pole–dipole array mode.

Taking coal seam thickness h, coal seam resistivity ρ_{m}, surrounding rock resistivity ρ_{w}, and other main parameters as variables, this paper designs three types of numerical models (Table 1) and analyzes the relationship of major parameters with the results obtained from the parallel coal seam detection method (Figures 7–9).

Experimental measurements of major parameters (Figures 7–9) revealed that: (1) the increase of coal seam thickness increases the thickness of the high-resistivity layer in shallow parts, the repulsion of the high-resistivity body to the current gradually weakens, raises apparent resistivity, and shields the anomaly response induced by collapse columns. Parallel coal seam detection methods can more effectively detect collapse columns in thin coal seams, compared to thick coal seams. (2) Variations in coal seam thickness only influence the observation results of a small polar distance, and with increasing coal seam resistivity, the apparent resistivity in shallow parts increases as well. (3) The resistivity difference between surrounding rock and anomalous bodies has a significant influence on the detection, and the decrease of such resistivity difference gradually weakens the anomaly response. The attraction of the low-resistivity body to the current decreases gradually. The electric difference between surrounding rock and anomalous bodies constitutes a physical premise of parallel coal seam detection methods.

5 Instance analysis

The parallel coal seam detection method is applied to practical engineering for detecting concealed geological structures in working faces. Taking the detection of collapse columns in working faces in a mine located in

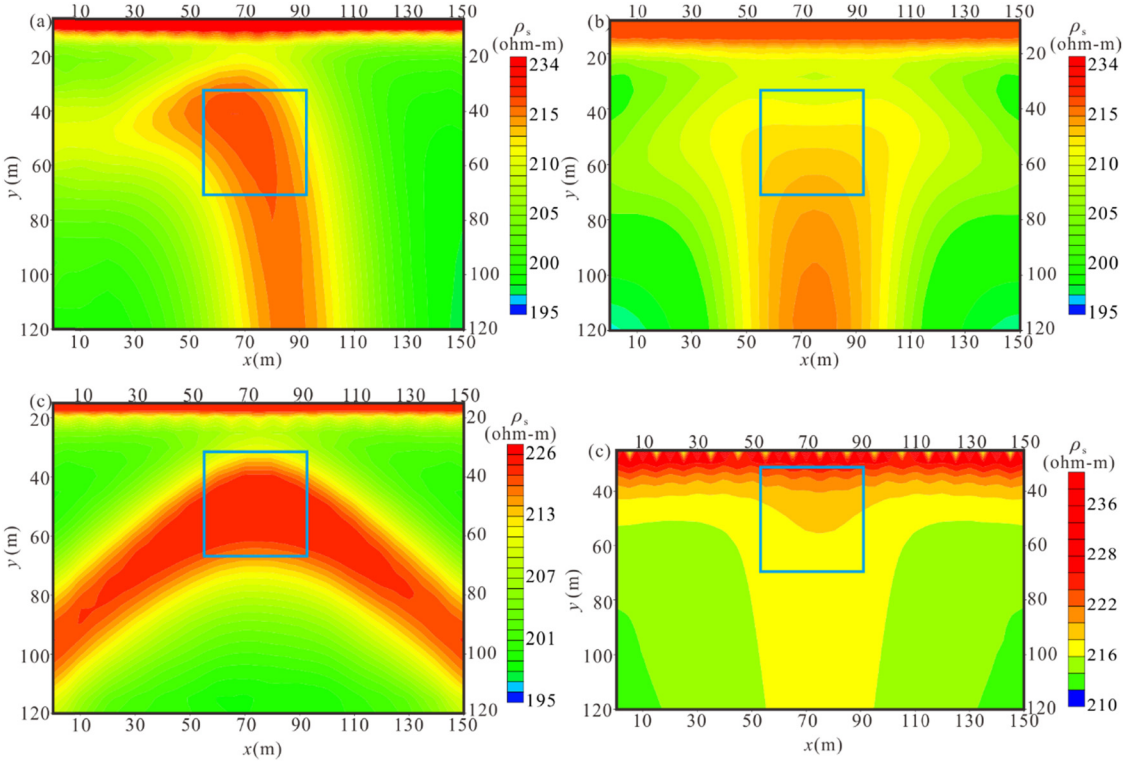

Figure 6: Apparent resistivity isolines of different observation systems. (a) Pole–dipole array; (b) Schlumberger array; (c) dipole–dipole array; (d) differential array.

Jiangsu Province as an example, this paper describes the practical application of the parallel coal seam detection method.

5.1 Construction design

During the cut-hole excavation from conveyor roadway to coal seam in the 92,606 working face of the mine in Jiangsu Province, a collapse column about 80 m away from the conveyor roadway was found. The collapse column was characterized by missing coal seam, incomplete lithology, and loose filler. Neither water burst nor water drenching was present. The preliminary judgment was that the collapse column was a non-water-flowing and non-water-bearing collapse column.

The 92,606 working face was about −750 m in elevation and 160 m in width; airway caved during the stoping of the adjacent working face; cut-hole had a high slope and lacked adequate support. To guarantee detection precision and construction safety, a consequent pole–dipole array detection system was designed, as shown in Figure 10. Fifty-one electrodes were arranged at cut-hole positions from left to right with an electrode spacing of 5 m (measuring line length = 250 m) and were connected with each other using a communication line; “infinite” electrodes were arranged about 1,000 m way from cut-holes along the roadway. Because of the high resistivity of coal seams and coal gangues, the electrode earthing resistance was high. To ensure the effectiveness of collected signals, holes 20–30 cm in depth were drilled at electrode locations, and wet clay

Table 1: Numerical model program

Program type	Invariable parameter	Variable parameter
Variable coal seam thickness type	ρ_m = 500 Ω m, ρ_w = 200 Ω m	h = 1, 2, 5, 8, 10, 15 m
Variable coal seam resistivity type	h = 5 m, ρ_w = 200 Ω m	ρ_m = 100, 200, 500, 800, 1,000, 1,500 Ω m
Variable surrounding rock resistivity type	h = 5 m, ρ_m = 500 Ω m	ρ_w = 200, 300, 500, 800, 1,000, 2,000 Ω m

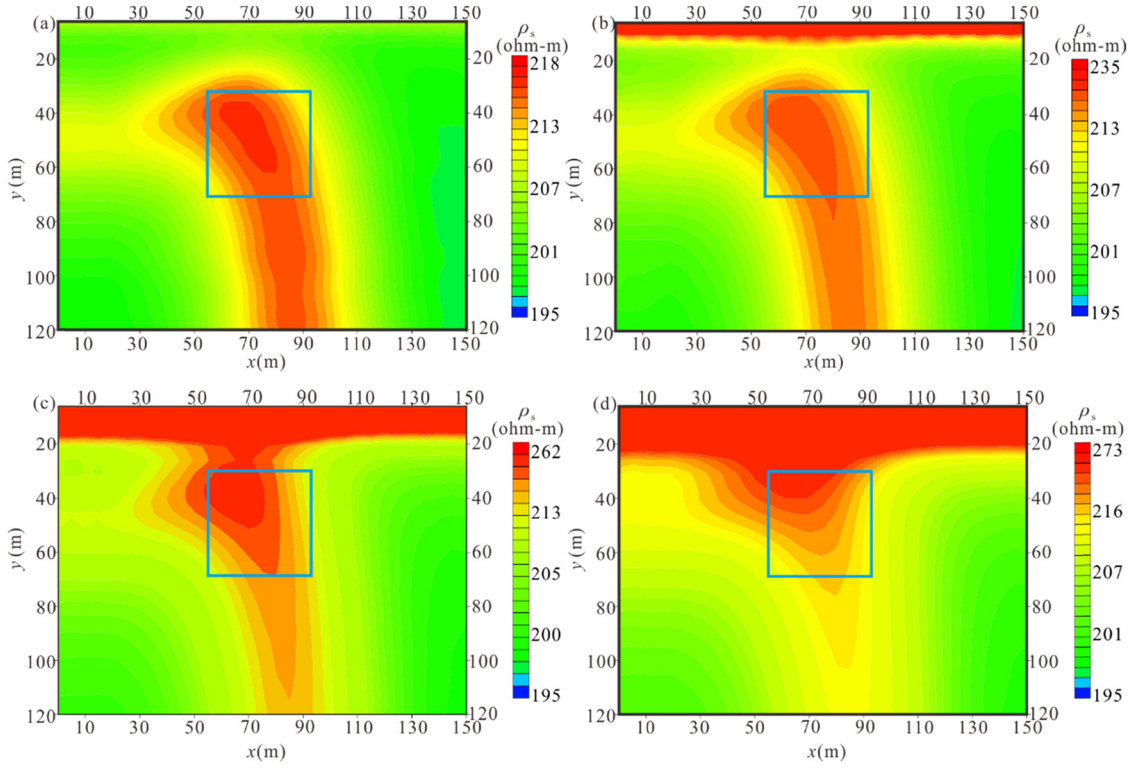

Figure 7: Apparent resistivity isolines of different coal seam thicknesses. (a) h = 1 m; (b) h = 5 m; (c) h = 10 m; (d) h = 15 m.

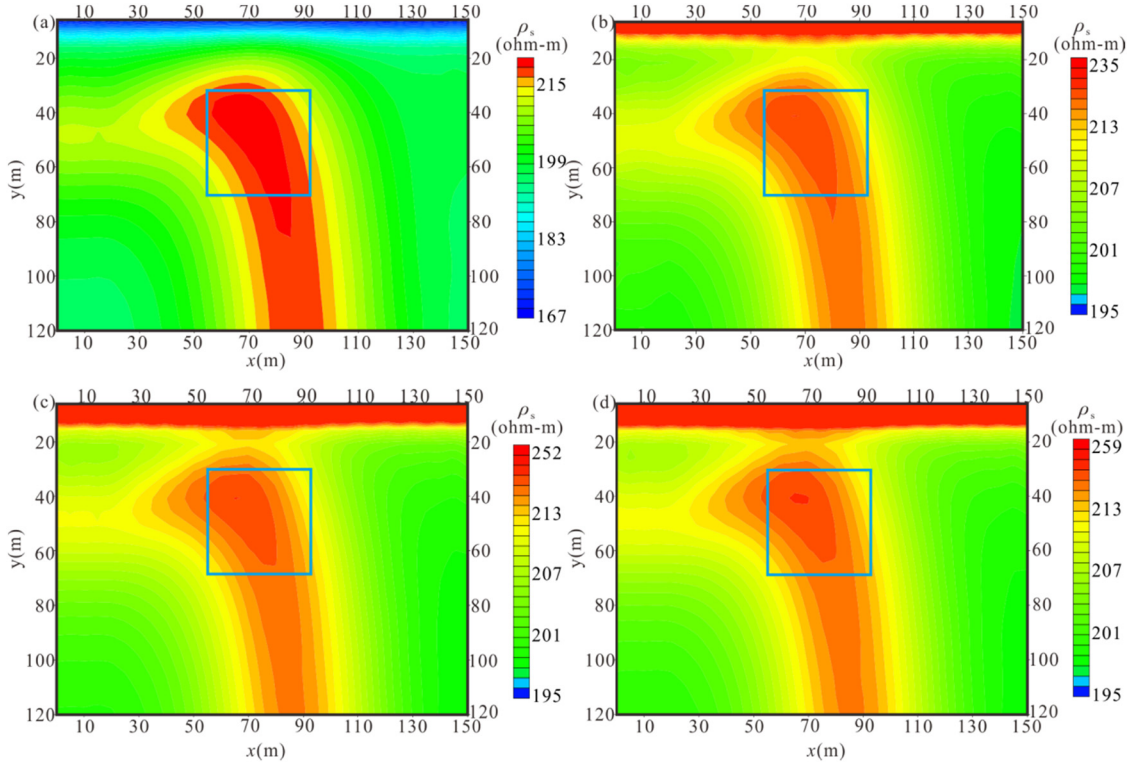

Figure 8: Apparent resistivity isolines of different coal seam resistivities. (a) ρ_m = 100 Ω m; (b) ρ_m = 500 Ω m; (c) ρ_m = 1,000 Ω m; (d) ρ_m = 1,500 Ω m.

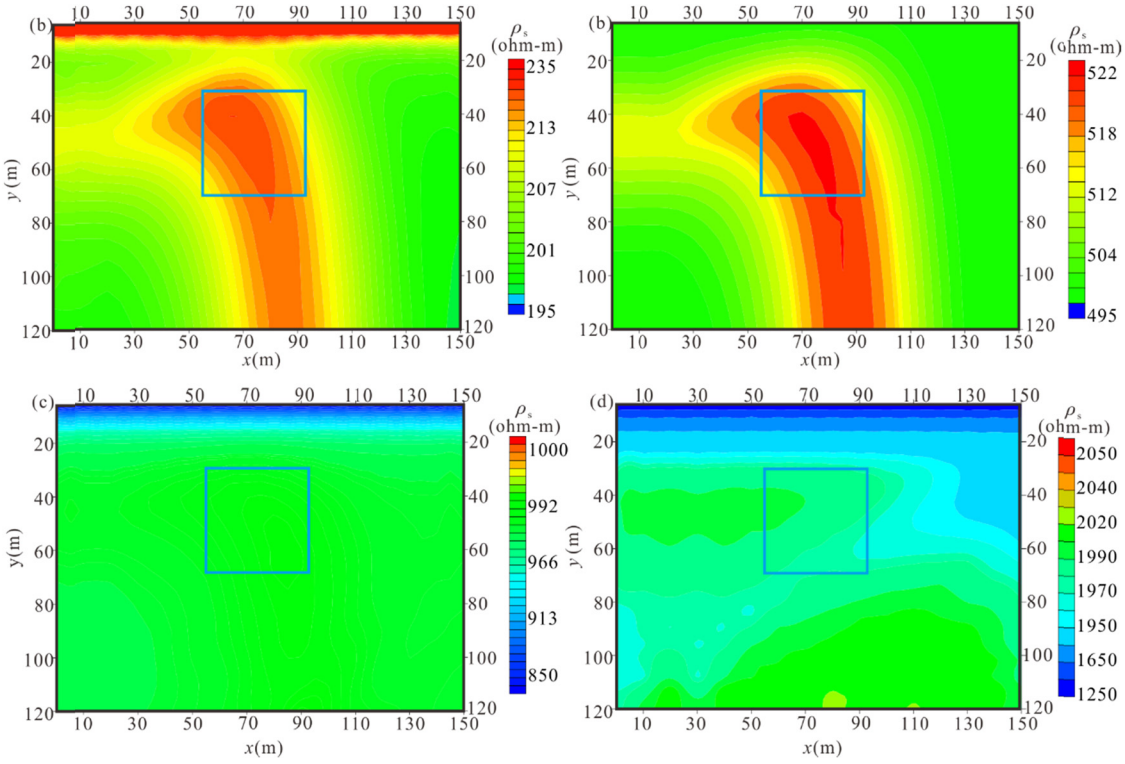

Figure 9: Apparent resistivity isolines of different surrounding rock resistivities. (a) ρ_w = 200 Ω m; (b) ρ_w = 500 Ω m; (c) ρ_w = 1,000 Ω m; (d) ρ_w = 2, 000 Ω m.

with an excellent electrical conductivity was stuffed inside.

5.2 Analysis of measured data

Data were collected using the parallel electrical survey-based system. Each electrode in the system was always kept in a voltage sampling state, except for the power supply; measured data, collected in large volumes, were transmitted to the host via the communication line in real time.

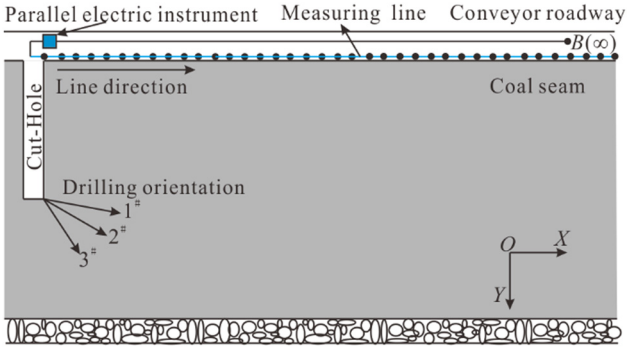

Figure 10: Schematic diagram of the resistivity observation system of the 92,606 working face.

After the conversion of field data, pole–dipole array data were extracted; on the basis of field measured data (roadway width = 6 m; roadway height = 5 m; coal seam resistivity = 700 Ω m, and surrounding rock resistivity = 250 Ω m), a geoelectric model was established, and the influence correction coefficient of the roadway cavity was obtained through a forward calculation. Measured data, after being corrected (Figure 11(a)), were put through smoothing and interpolation processing, and apparent resistivity isolines were drawn, Figure 11(b). Experimental measurements of the pole–dipole array are given in Figure 11(b). These results revealed that, at a longitudinal depth of 20–30 m, the apparent resistivity was generally low, which was conjectured to be a consequence of the roadway floor ponding and not interpreted as an anomaly. At a transverse position of 5–60 m and a longitudinal depth of 80–150 m (area demarcated by blue dotted lines), the apparent resistivity was high, which was conjectured to be a high anomaly response induced by non-water-flowing and non-water-bearing collapse columns. At a transverse position of 80–100 m and a longitudinal depth of 30–70 m (area demarcated by red dotted lines), the

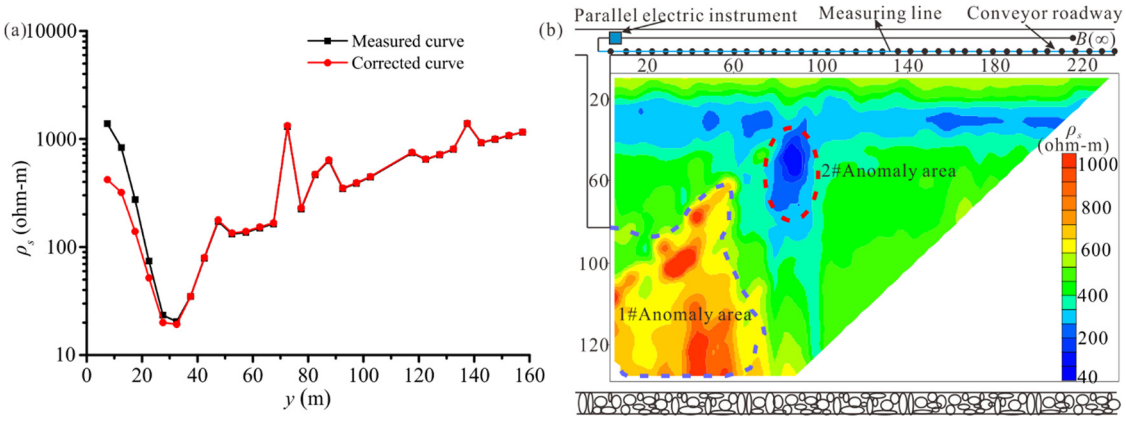

Figure 11: Observation results of the pole–dipole array. (a) Apparent resistivity curves (x = 47.5 m) and (b) apparent resistivity isolines.

apparent resistivity was low and presented a zonal distribution, which was conjectured to be a fault. The detection results fit well with the drilling verification results obtained by the mine owner and deviated from the actual collapse column position by about 3 m, which could meet the production demands of the mine owner.

6 Conclusions

(1) According to the electric field distribution characteristics of artificial field sources in coal strata, this paper proposes a parallel coal seam detection method that arranges observation systems in coal seams to detect concealed geological structures.

(2) Roadway cavities have a significant influence on the measurement results of small polar distance in parallel coal seam detection methods. Because of current shielding by roadway cavities, the majority of current flows into coal seams, which enhances the ability of parallel coal seam detection methods to detect anomalous bodies in coal seams.

(3) The consequent pole–dipole (A-MN) observation system is the most ideal in terms of dividing the geoelectric interfaces of concealed geological structures in working faces, and its detection effect is influenced significantly by the coal seam thickness and the electric difference between surrounding rock and anomalous bodies. Coal seam resistivity slightly influences detection of the consequent pole–dipole system.

(4) According to practical application effects, the parallel coal seam detection method can solve the problem of detecting concealed geological structures in "single-roadway" working faces.

Acknowledgments: This study is funded by "the National Key R&D Program of China (Grant No. 2018YFC0807802-3)" and "A Project Funded by the Priority Academic Program Development of Jiangsu Higher Education Institutions (PAPD)."

References

[1] Lu T, Liu SD, Wang B, Wu RX, Hu XW. A review of geophysical exploration technology for mine water disaster in China: applications and trends. Mine Water Environ. 2017;5:1–10.

[2] Krishnamurthy NS, Rao VA, Kumar D, Singh KKK, Ahmed S. Electrical resistivity imaging technique to delineate coal seam barrier thickness and demarcate water filled voids. J Geol Soc India. 2009;5:639–50.

[3] Maillol JM, Seguin MK, Gupta OP, Akhauri HM, Sen N. Electrical resistivity tomography survey for delineating uncharted mine galleries in West Bengal, India. Geophys Prospect. 2010;2:103–16.

[4] Bharti AK, Pal SK, Priyam P, Kumar S, Srivastava S. Subsurface cavity detection over Patherdih colliery, Jharia Coalfield, India using electrical resistivity tomography. Environ Earth Sci. 2016;5:1–17.

[5] Danielsen JE, Auken E, Jørgensen F, Søndergaard V, Sørensen KI. The application of the transient electromagnetic method in hydrogeophysical surveys. J Appl Geophysics. 2003;4:181–98.

[6] Shi L, Wang Y, Qiu M, Gao W, Zhai P. Application of three-dimensional high-density resistivity method in roof water advanced detection during working stope mining. Arab J Geosci. 2019;15. doi: 10.1007/s12517-019-4586-7.

[7] Xue GQ, Yu JC. New development of TEM research and application in coal mine exploration. Prog Geophys. 2017;1:319–26.

[8] Zhao GM, Li T, Xu KJ, Li JP. The study and application of well-surface resistivity method in the safety at coal field. Prog Geophys. 2007;6:1895–9.

[9] Jiao XF, Jiang ZH, Liu SC. Exceptional response characters of radio wave perspective in coal thinning zone. J Min Saf Eng. 2014;6:1001–4.
[10] Yang ST, Wei JC, Cheng JL, Shi LQ, Wen ZJ. Numerical simulations of full-wave fields and analysis of channel wave characteristics in 3-D coal mine roadway models. Appl Geophys. 2016;4:621–30.
[11] Hu ZA, Zhang P, Xu G. Dispersion features of transmitted channel waves and inversion of coal seam thickness. Acta Geophys. 2018;5:1001–9.
[12] Li D, Han DP, Shi YD, Shi XF. A DC electrical penetration method for prospecting the coal face alone the same coal layer. J China Coal Soc. 2010;8:1336–40.
[13] Bryn H, Andrew B, Lee S, Roy M, Bernd K. Inter-borehole electrical resistivity imaging of englacial drainage. J Glaciol. 1998;147:429–35.
[14] Hu Z, Zhang P, Xu G. Dispersion features of transmitted channel waves and inversion of coal seam thickness. Acta Geophys. 2018;5:1001–9.
[15] Zhu M, Cheng J, Cui W, Yue H. Comprehensive prediction of coal seam thickness by using in-seam seismic surveys and Bayesian kriging. Acta Geophys. 2019;4:1–12.
[16] Ge M, Wang H Jr, Hardy HR, Ramani R. Void detection at an anthracite mine using an in-seam seismic method. Int J Coal Geol. 2008;3–4:201–12.
[17] Chang JH, Yu JC, Liu ZX. Three-dimensional numerical modeling of full-space transient electromagnetic responses of water in goaf. Appl Geophys. 2016;3:539–52.
[18] Cheng JL, Li F, Peng SP, Sun XY. Research progress and development direction on advanced detection in mine roadway working face using geophysical methods. J China Coal Soc. 2014;8:1742–50.
[19] Yue JH, Liu SC, Liu ZX, Wang DQ, Wu J. Application of roadway DC electrical sounding in detecting collapse-columns. J China Univ Min Technol. 2003;5:13–15.
[20] Su BY, Yu JC, Li MF. Research on algorithm of borehole resistivity imaging method. Tehnički Vjesn. 2017;3:817–20.
[21] Das P, Pal SK, Mohanty PR, Priyam P, Bharti AK. Abandoned mine galleries detection using electrical resistivity tomography method over Jharia coal field, India. J Geol Soc India. 2017;2:169–74.
[22] Yue JH, Li ZD, Mine DC. Electrical methods and application to coal floor water invasion detecting. J China Univ Min Technol. 1997;1:96–100.
[23] Liu SC, Liu XM, Jiang ZH, Xing T, Chen MZ. Research on electrical prediction for evaluating water conducting fracture zones in coal seam floor. Chin J Rock Mech Eng. 2009;02:348–56.
[24] Zhang L, Ruan B, Lv Y, Yang T, Chen W. Study of full-space numerical modeling of advanced exploration in tunnel with DC focus resistivity method. Chin J Geo Phys. 2011;4:1130–9.
[25] Gyulai Á, Ormos T, Turai E, Sasvári T. In-mine geoelectric investigations for detecting tectonic disturbances in coal seam structures. Acta Geophys. 2013;5:1184–95.
[26] Plank Z, Polgar D. Application of the DC resistivity method in urban geological problems of karstic areas. Surf Geophysics. 2019;5:547–61.
[27] Gallardo LA, Meju MA. Joint two-dimensional DC resistivity and seismic travel time inversion with cross-gradients constraints. J Geophys Res Solid Earth. 2004;B3:B03311.
[28] Spitzer K. A 3-D finite-difference algorithm for DC resistivity modelling using conjugate gradient methods. Geophys J Int. 2007;3:903–14.